

Pd stabilized on nanocomposite of halloysite and β -cyclodextrin derived carbon: An efficient catalyst for hydrogenation of nitroarene

Samahe Sadjadi^{a,*}, Fatemeh Ghoreyshi Kahangi^b, Majid M. Heravi^c

^a Gas Conversion Department, Faculty of Petrochemicals, Iran Polymer and Petrochemicals Institute, PO Box 14975-112, Tehran, Iran

^b Department of Chemistry, University Campus 2, University of Gilan, Rasht, Iran

^c Department of Chemistry, School of Science, Alzahra University, PO Box 1993891176, Vanak, Tehran, Iran

ARTICLE INFO

Article history:

Received 29 June 2019

Accepted 27 October 2019

Available online 1 November 2019

Keywords:

β -Cyclodextrin

Nanospheres

Halloysite

Heterogeneous catalysts

Hydrogenation

ABSTRACT

Carbon nanospheres, CCDs, were fabricated using β -cyclodextrin as carbon precursor. The as prepared CCD was then hybridized with halloysite nanotubes (Hal) through hydrothermal treatment to furnish a nanocomposite, Hal-CCD that was subsequently applied as support to stabilize Pd nanoparticles. Investigation of the catalytic activity of palladated nanocomposite, Pd@Hal-CCD, for the hydrogenation reaction of nitrobenzenes confirmed that Pd@Hal-CCD could efficiently promote the hydrogenation reaction under mild reaction condition. Moreover, the catalyst was recyclable and showed slight Pd leaching upon reusing. The comparison of the catalytic activity of Pd@Hal-CCD with that of Pd@Hal and Pd@CCD indicated the superior catalytic activity of the former. The observed high catalytic activity of the catalyst was attributed to its higher Pd loading and water disperse ability. Additionally, the results confirmed that the ratio of Hal:CCD could affect the catalytic activity and the best result was obtained by using Hal:CCD ratio of 1:2.

© 2019 Elsevier Ltd. All rights reserved.

1. Introduction

In recent years, utilization of natural halloysite nanotubes (Hal) in diverse fields of research such as catalysis and drug delivery witnessed tremendous growth [1–8]. This issue is due to the remarkable physicochemical properties of Hal such as high thermal and mechanical stability, availability, non-toxicity and more importantly, its tubular morphology that allows Hal to encapsulate various guest molecules [2,9–11]. For catalytic purposes, the promising results have been achieved when Hal was surface modified or applied in combination with other materials in hybrid or composite forms [12–14]. In this context various catalytic composites of Hal such as Hal-dendrimer, Hal-polymers and Hal-carbon materials have been reported [14].

Among oligosaccharides, cyclodextrins (CDs) that possess cyclic structures have received considerable attention due to their unique properties, i.e. having a hydrophilic exterior surface and hydrophobic cavity [15–18]. The interior cavity of CD can be exploited to host diverse range of molecules such as biologically active species.

Using host-guest chemistry of CD, various state of the art catalysts can be designed and developed for performing the reaction in aqueous media [18–20]. On the other hand, CDs can be considered as potent carbon precursors to form carbon materials [21–23].

Synthesis of anilines through reduction of nitro compounds is a utile reaction, applicable for the production of more sophisticated chemicals [24]. This hydrogenation reaction is mostly promoted by precious metal-based catalysts in the presence of hydrogen gas or chemical reducing agent. To render this chemical transformation more economic and environmentally benign, the precious metals are mostly stabilized on supports. Considering the importance of catalyst support on the catalytic performance and recyclability of the catalyst, development of efficient supports that prevent from coverage of catalyst active sites and/or exert catalytic activity is of great importance [25–29].

In the continuation of our efforts on disclosing the application of Hal for the catalytic purposes [12,30–32], herein we wish to report a novel nanocomposite based on hydrothermal treatment of Hal with carbon nanospheres derived from CD as carbon precursor. To furnish this nanocomposite, Hal-CCD, the CCD was first prepared through hydrothermal treatment of CD followed by carbonization under inert atmosphere. Subsequently, CCD was treated with Hal under hydrothermal condition to furnish Hal-CCD. In the next part of this research, Hal-CCD was utilized as support for the immobilization of Pd nanoparticles. The resulting

* Corresponding author at: Gas Conversion Department, Faculty of Petrochemicals, Iran Polymer and Petrochemicals Institute, PO Box 14975-112, Tehran, Iran. Tel.: 982148666; fax: +982144787021-3.

E-mail addresses: s.sadjadi@ippi.ac.ir, samahesadjadi@yahoo.com (S. Sadjadi), m.heravi@alzahra.ac.ir (M.M. Heravi).

nanocomposite, Pd@Hal-CCD was then employed as a catalyst for promoting hydrogenation of nitrobenzene under mild reaction condition. The role of CCD and Hal in the catalysis and the effect of Hal:CCD ratio on the catalysis as well as the recyclability of the catalyst were also investigated.

2. Experimental

2.1. Materials and instruments

The chemicals used for the synthesis of the catalyst and performing the catalytic experiments included nitrobenzene, 1-nitronaphthalene, hydrogen gas, EtOH, toluene, Pd(OAc)₂, NaBH₄, 4-nitroacetophenone, Hal, β-CD and deionized water, all purchased from Sigma-Aldrich and used as received without further purification.

Catalyst characterization was carried out by applying various techniques, including XRD, BET, TGA, FTIR, TEM, SEM and ICP-AES. XRD patterns of CCD, Hal and Pd@Hal-CCD were obtained by using a Siemens, D5000. Cu Kα radiation from a sealed tube. The BET analyses of the final catalyst and pristine Hal were performed using BELSORP Mini II instrument. To perform the BET analysis, the required amount of the samples were pre-heated at 150 °C for 2 h. To study the thermal stability of the catalyst and some prepared compounds, METTLER TOLEDO thermogravimetric analysis apparatus was employed. The thermograms of the samples were recorded under N₂ atmosphere. The used heating range and rate were 50–800 °C and 10 °C min⁻¹ respectively. The FTIR spectra of Pd@Hal-CCD and other samples were recorded by employing PERKIN-ELMER Spectrum 65 instrument. The metal loading of Pd@Hal-CCD as well as its leaching in the course of recycling were estimated by using ICP analyzer (Varian, Vista-pro). FESEM/EDS images were obtained by applying a Tescan instrument, using Au-coated samples and acceleration voltage of 20 kV. Transmission electron microscope (TEM) images of Pd@Hal-CCD were recorded with a CM30300Kv field emission transmission electron microscope.

2.2. Catalyst preparation

2.2.1. Synthesis of CCD

The CCD nanospheres were synthesized by a facile hydrothermal process followed by a two-step heat treatment [33]. Typically, 10.0 g β-CD in aqueous solution was placed into 150 mL Teflon sealed autoclave and maintained at 200 °C for 12 h and then cooled to the room temperature. Subsequently, the precipitate was filtered off and washed with distilled water several times and dried in oven at 80 °C for 12 h. Then, the collected precursor was carbonized at 800 °C for 2 h under N₂ atmosphere. Finally, the obtained product was further annealed at 400 °C for 1.5 h in air for activation.

2.2.2. Synthesis of Hal-CCD

To prepare Hal-CCD nanocomposite, Hal and CCD with weight ratio of 1:2 were mixed in distilled water and then transferred into a 150 mL Teflon-lined stainless steel autoclave. The reactor was sealed and maintained at 220 °C for 48 h. After hydrothermal treatment, the nanocomposite was filtered off and after washing with distilled water dried in oven at 60 °C in 24 h.

2.2.3. Synthesis of Pd@Hal-CCD

Immobilization of Pd nanoparticles on Hal-CCD nanocomposites, was accomplished by wet impregnation method. Briefly, a solution of 0.02 g Pd(OAc)₂ in toluene was added to the suspension of 1 g Hal-CCD dispersed in dry toluene (17 mL). The mixture was

then stirred at room temperature for 3 h. In the next step, a solution of 0.075 g NaBH₄ in 10 mL water was added into the Hal-CCD and Pd(OAc)₂ suspension in a dropwise manner and the resulting mixture was stirred for 2 h. Finally, the solid material was filtered off, washed with water and dried in oven at 60 °C for 12 h. The schematic procedure of the synthesis of the catalyst is illustrated in Fig. 1.

Pd loading of Pd@Hal-CCD was measured via ICP-AES analysis. The sample preparation procedure for ICP analysis is as follow: a mixture (1:3) of concentrated nitric acid and hydrochloric acid was prepared and Pd@Hal-CCD (0.02 g) was digested in the aforementioned acidic solution through constant stirring for 24 h. Subsequently, the resulting extract was analyzed by ICP-AES. The Pd content of the catalyst was measured to be about 0.28 wt%.

2.2.4. Synthesis of control samples

To shed light to the roles of CCD and Hal in the catalysis, two control samples, Pd@Hal and Pd@CCD were prepared via the reported procedure for preparing the catalyst, except, Hal and CCD were applied as supports respectively. To investigate the effect of ratio of Hal:CD, apart from the main catalyst (Pd@Hal-CCD (1:2)), two other samples with different ratios of Hal:CCD, Pd@Hal-CCD (1:1) and Pd@Hal-CCD (2:1), were fabricated with a similar method, except with use of Hal:CCD ratios of 1:1 and 2:1 respectively.

2.3. Hydrogenation of nitroarene

In a typical reaction, Pd@Hal-CCD catalyst (1 wt%) and nitroarene compound (1 mmol) in deionized water as solvent (2 mL) were placed in the reaction vessel. Then, hydrogen (1 bar) as reducing agent was purged into the stirring reaction mixture at room temperature for 1.5 h. Upon completion of the reaction (monitored by TLC), the reaction was held and Pd@Hal-CCD was separated from the reaction mixture and the corresponding aniline was isolated by evaporation of water. To recycle Pd@Hal-CCD, the recovered catalyst was washed with water and EtOH several times, then dried in oven at 80 °C for 8 h. All the obtained products were known and their formation was verified by using FTIR, GC-Mass and comparing their melting/boiling points with that of authentic samples, see "Supporting Information".

3. Results and discussion

First, the formation of CCD was confirmed by recording its specific surface area, FESEM images, XRD pattern and FTIR spectrum, Fig. 2. The FESEM images, Fig. 2 A and B, showed the spherical morphology of the prepared CCD. In the FTIR spectrum of CCD, Fig. 2 D, several characteristic bands, including the bands at 3438 cm⁻¹ (–OH), 1656 cm⁻¹ (–C=O) can be observed, indicating that CCD contained oxygenated functionalities. The XRD pattern of CCD, Fig. 2C, exhibited a broad band at 2θ = 25° and a sharp band at 2θ = 36°. This pattern is in a good agreement with the previous report, in which these bands were attributed to the (0 0 2) and (1 0 0) reflections of the graphitic framework, JCPDSno.04-0850 [33]. Using BET, the specific surface area of CCD was calculated to be 561 m² g⁻¹.

Following the successful fabrication of CCD, it was studied whether CCD in its free form has any catalytic activity for promoting hydrogenation reaction of nitrobenzene. To this purpose, the hydrogenation reaction in water as solvent, in the presence of H₂ gas (1 bar) and CCD (1 wt%) as catalyst was performed at room temperature. The result confirmed that even after passing 1.5 h no desired product, aniline, was furnished, confirming that bare



Fig. 1. The schematic protocol for the synthesis of Pd@Hal-CCD.

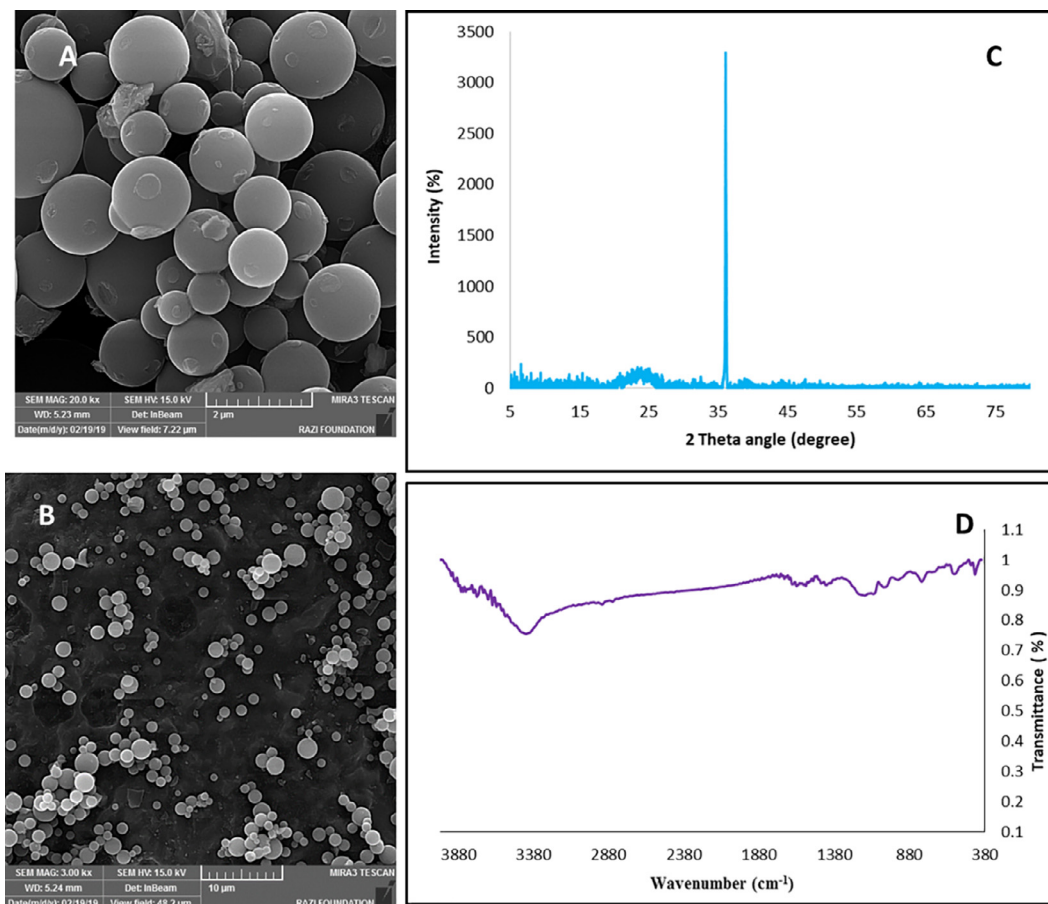


Fig. 2. A and B, the FESEM images, C, the XRD pattern and D the FTIR spectrum of the prepared CCD.

CCD was not catalytically active for this reaction. Next, CCD was palladated (Experimental section) and applied as a catalyst under similar reaction condition. The result, Table 1, confirmed that Pd@CCD showed slight catalytic activity and led to 30% aniline.

Considering the promising results of our previous studies on the catalytic activity of Hal-carbon nanocomposites [12], it was investigated whether incorporation of Hal could improve the catalytic activity of CCD. In this line, hybrid of Hal-CCD (1:2) was prepared and then palladated (Experimental section). The prepared catalyst

was first characterized via XRD, FTIR, BET, TGA and TEM techniques.

In Fig. 3 the FTIR spectrum of Pd@Hal-CCD (1:2) is depicted and compared with that of Hal and CCD (the FTIR spectrum of CCD is discussed previously and provided here for comparison). As shown the FTIR spectrum of the catalyst is very similar to that of CCD and showed the characteristic bands of CCD at 3463 and 1656 cm^{-1} . Comparing the FTIR spectrum of Pd@Hal-CCD (1:2) with that of pristine Hal, it can be concluded that in the FTIR spectrum of the

Table 1

Comparison of catalyst activity of various catalysts developed in this study for THE hydrogenation of nitrobenzene.^a

Entry	Catalyst	Yield (%) ^b
1	CCD	0
2	Pd@CCD	30
3	Pd@Hal	20
4	Pd@Hal-CCD (1:1)	80
5	Pd@ Hal-CCD (2:1)	60
6	Pd@ Hal-CCD (1:2)	100
7	Hal/Pd@CCD	30

^a Reaction condition: Benzyl alcohol (1 mmol), catalyst (1 wt%), H₂O (2 mL), H₂ (1 bar), agitation (400 rpm) at r.t. in 1.5 h.

^b Isolated yields.

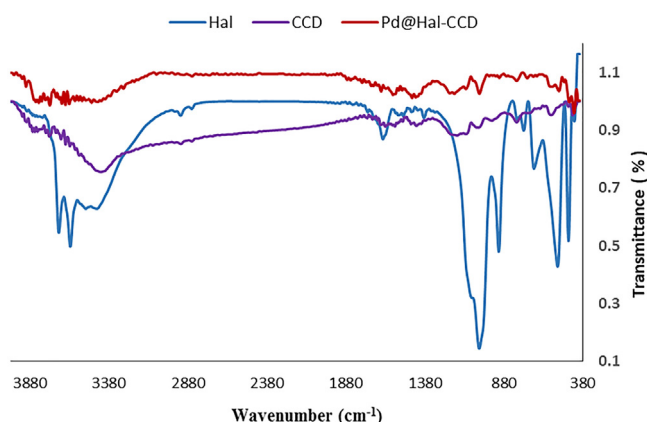


Fig. 3. FTIR spectra of CCD, Hal and Pd@ Hal-CCD (1:2).

catalyst the characteristic bands of Hal can be observed, i.e. the bands at 580 cm⁻¹ (Al-O-Si vibration), 1035 cm⁻¹ (Si-O stretching), 3695 and 3622 cm⁻¹ (internal -OH). However, their intensities significantly reduced in the hybrid system.

In Fig. 4 the XRD patterns Hal and Pd@Hal-CCD (1:2) are illustrated. According to the literature, the Hal distinctive peaks are appeared at $2\theta = 12.3^\circ, 20.6^\circ, 25.2^\circ, 36.7^\circ, 39.0^\circ, 56.3^\circ$ and 62.5° (JCPDS No. 29-1487, labeled as *) [34]. Comparing the XRD pattern of the Pd@Hal-CCD (1:2) with that of Hal, it was found that in the XRD pattern of the catalyst the Hal peaks are present. However, the intensities of those peaks remarkably reduced. It is worth mentioning that in the XRD pattern of Pd@Hal-CCD (1:2), the Hal peaks were in the same position of pristine Hal with no displacement.

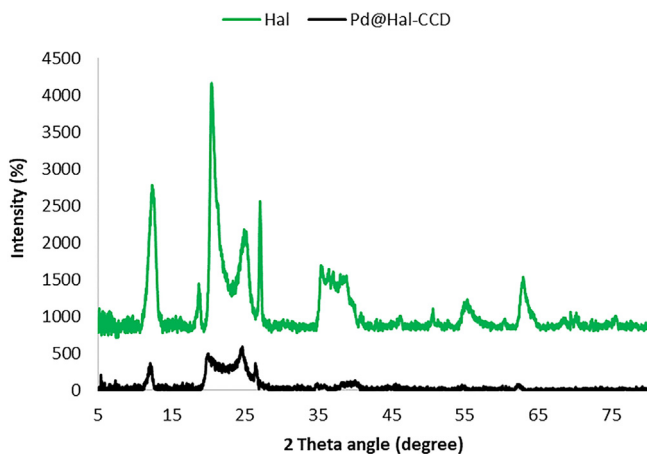


Fig. 4. XRD patterns of Hal and Pd@ Hal-CCD (1:2).

This issue confirmed the fact that the tubes of Hal are preserved in the Pd@Hal-CCD (1:2). On the other hand, the two characteristic peaks of CCD, Fig. 2 C, overlapped with those of Hal. Hence, the presence of CCD can be confirmed by other analyses such as TGA (vide infra). The characteristic peaks of Pd in Pd@Hal-CCD (1:2) was not observed. This issue can be justified by small particle size of well-dispersed Pd nanoparticles (see the TEM images).

The measurement of the specific surface area of Pd@Hal-CCD (1:2) was accomplished using BET method. This value was estimated to be 109.15 cm³ g⁻¹. Notably, the specific surface area of Pd@Hal-CCD (1:2) was higher than that of pristine Hal (~52 cm³ g⁻¹) and lower than that of CCD (561.3 cm³ g⁻¹).

The morphology of Pd@Hal-CCD (1:2) was studied by recording its TEM images, Fig. 5. The TEM images showed the tubes of Hal, indicating that Hal maintained its structure in the course of hydrothermal treatment with CCD. This issue was previously reported the literature [35]. The tiny black spots in the TEM are representative of Pd nanoparticles (mean particle diameter of 4 nm). The potential of Pd species for coordination on the surface of the support is reported previously [36]. As shown, the Pd nanoparticles were well dispersed and no aggregation was observed. The TEM images also showed that Hal tubes are covered to some extent with CCD. However, in the recorded TEM images, the spherical morphology of CCD was not no longer detectable.

The thermograms derived from TG analysis of Pd@ Hal-CCD (1:2) and pristine Hal are illustrated in Fig. 6. As shown, the pristine Hal mass losses occurred at ~150 °C (loss of water) and ~500 °C (dehydroxylation) [37,38]. The thermogram of Pd@Hal-CCD (1:2) showed an additional loss step due to the presence of CCD, the loss goes from 540 °C to 800 °C showing a 13% of weight loss.

Confirming the formation of Pd@Hal-CCD (1:2), its catalytic activity for the hydrogenation of nitrobenzene was studied. First, the effects of reaction variables, including reaction temperature, solvent and catalyst amount were investigated, Table S1. In the first try, the reaction was performed in water as environmentally benign solvent at room temperature and in the presence of very low amount of the catalyst (1 wt%). Gratifyingly, the catalytic tests showed Pd@Hal-CCD (1:2) led to 100% aniline after 1.5 h. To investigate whether increase of the reaction time could accelerate the reaction, the model hydrogenation reaction was repeated at 50 °C. Tracing the reaction at short time intervals, it was found out that increase of temperature accelerated the reaction and the reaction reached to 80% conversion and yield after 1 h. However, the reaction kinetic slowed down and after 1.5 h quantitative yield and conversion were achieved. Therefore, the optimum reaction temperature was found to be ambient temperature. Regarding catalyst amount, examining the reaction using higher catalyst amount showed that increase of the catalyst had no effect on the time and yield of the reaction, while use of lower catalyst loading led to lower yield and conversion. Although water as solvent proved to be efficient, the efficiencies of some other conventional solvents, including EtOH, CH₃CN, H₂O:EtOH (1:1), THF and toluene were also examined. The results confirmed that water resulted in the best catalytic performance. Noteworthy, the disperse ability of the catalyst in water was better than other solvents. Hence, it was selected as an environmentally benign solvent for the reaction.

Then, the catalytic activity of the catalyst was compared with that of Pd@Hal and Pd@CCD. It is worth noting that Hal in its individual form was not a suitable support for Pd nanoparticles and the catalytic activity of Pd@Hal was very low (20%). Notably, the disperse ability of Pd@Hal was lower compared to that of the catalyst.

To shed light to the origin of high catalytic activity of Pd@Hal-CCD, the Pd loading and specific surface area of Pd@Hal and Pd@CCD were obtained and compared with those of the catalyst. The specific surface area of these samples decreased in the order

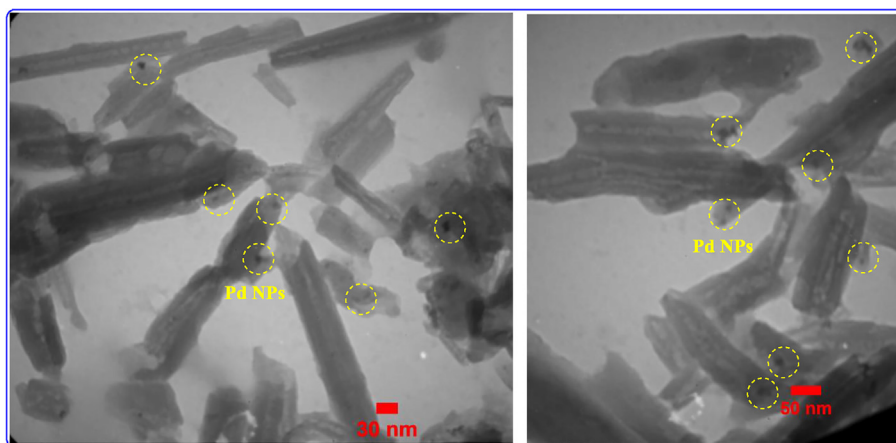


Fig. 5. The TEM images of Pd@Hal-CCD (1:2).

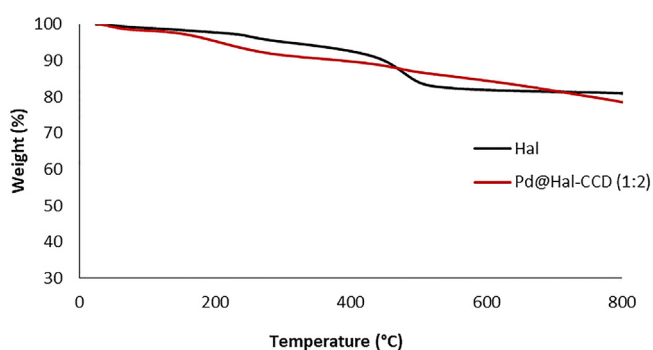


Fig. 6. The thermogram of Pd@Hal-CCD (1:2) and pristine Hal.

of Pd@CCD ($\sim 450 \text{ m}^2 \text{ g}^{-1}$) > Pd@Hal-CCD ($\sim 109 \text{ m}^2 \text{ g}^{-1}$) > Pd@Hal ($\sim 40 \text{ m}^2 \text{ g}^{-1}$). The order of decrease of loading of Pd was as follow: Pd@Hal-CCD (0.28 wt%) > Pd@Hal (0.22 wt%) > Pd@CCD (0.19 wt%).

According to the literature, pristine Hal cannot effectively stabilize Pd nanoparticles [11] and led to the immobilization of Pd nanoparticles with high average particle sizes. Moreover, low specific surface area of this sample ($\sim 40 \text{ m}^2 \text{ g}^{-1}$) can contribute to this observation. The low catalytic activity of Pd@CCD can be attributed to its lower Pd loading. Moreover, low disperse ability of this sample in aqueous media can justify its low catalytic activity. Regarding Pd@Hal-CCD, higher loading of Pd nanoparticles as well as its improved wet ability and water disperse ability can rationalize its higher catalytic activity. Considering the previous reports, the synergism between Hal and carbon material can be expected in the case of Pd@Hal-CCD [39].

Encouraged by the positive effect of hybridization of Hal and CCD, the role of Hal:CCD ratio in the catalytic activity of the final catalyst was elucidated by comparing the catalytic activity of Pd@Hal-CCD (1:2) with that of Pd@Hal-CCD (1:1) and Pd@Hal-CCD (2:1), Table 1. As tabulated, decreasing the content of CCD (confirmed by TG analysis) had a detrimental effect on the catalytic activity of the catalyst, indicating the contribution of CCD to the catalysis and importance of use of optimum ratio of Hal:CCD.

In the following, it was investigated whether hybridization of palladated CCD (Pd@CCD) with Hal (Hal/Pd@CCD) will result in a similar effect. Interestingly, it was found that the catalytic activity of Hal/Pd@CCD was similar to that of Pd@CCD and far lower than that of Pd@Hal-CCD (1:2). This issue can be attributed to the lower Pd loading of this sample (confirmed by ICP) compared to that of Pd@Hal-CCD.

Finding the best catalytic nanocomposite, it was investigated whether Pd@Hal-CCD (1:2) could catalyze the reaction of other nitroarenes. First, hydrogenation of 4-nitroacetophenone was examined to see whether the presence of competing functional group (here $-\text{C}=\text{O}$) could intervene the hydrogenation of nitro group. The result showed that the catalyst was 100% selective towards hydrogenation of nitro group and $-\text{C}=\text{O}$ functionality was not hydrogenated under the reaction condition and the only product was 4-aminoacetophenone. However, the conversion for this catalyst was lower and reached to 70%. The second substrate was 1-nitronaphthalene that was steric compared to nitrobenzene. The result, Table 2, confirmed that the catalyst could successfully promote the hydrogenation of sterically demanding substrates. Then, to confirm the generality of the developed protocol, the hydrogenation of some other nitroarenes with electron withdrawing and electron donating functional groups was examined. As tabulated, nitroarenes with different electron densities could tolerate the hydrogenation reaction under Pd@Hal-CCD catalysis to furnish the corresponding products in good to excellent yields. However, the substrates with electron withdrawing groups were more active and led to higher reaction yields.

In the following to elucidate whether the efficiency of Pd@Hal-CCD is comparable with the previously reported catalysts, the reaction condition and performance of Pd@Hal-CCD for the hydrogenation of nitrobenzene were compared with some of the reported procedures and catalysts, Table 3. As depicted, hydrogenation of nitrobenzene was reported in the presence of various catalysts and reducing agents. Among various reducing agents, hydrogen gas is more appealing compared to chemical reducing agents in

Table 2
Hydrogenation of nitro compound by Pd@Hal-CCD.^a

Entry	Substrate	Yield (%) ^b
1	Nitrobenzene	100
2	1-Nitronaphthalene	90
3	4-Nitroacetophenone	70
4	4-Nitroaniline	85
5	1-Bromo-2-nitrobenzene	92
6	1-Bromo-4-nitrobenzene	93
7	1-Chloro-2-nitrobenzene	95
8	1-Chloro-4-nitrobenzene	96
9	4-Nitrotoluene	89
10	2-Nitrotoluene	85

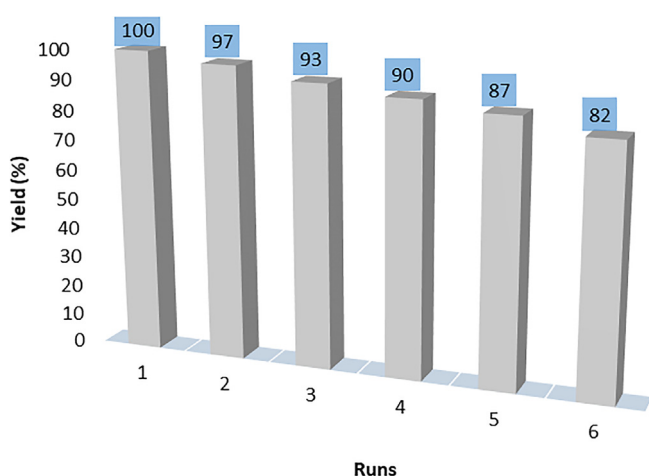
^a Reaction condition: Substrate (1 mmol), catalyst (1 wt%), H₂O (2 mL), agitation (400 rpm) at r.t and H₂ pressure of 1 bar in 1.5 h

^b Isolated yields.

Table 3

The comparison of the catalytic activity of Pd@Hal-CCD for the hydrogenation of nitrobenzene with that of some the catalysts in the literature.

Entry	Catalyst	Time	Solvent	Temperature (°C)	Reducing agent	Yield (%)	Ref.
1	Pd@Hal-CCD (1.wt.%)	1.5 h	H ₂ O	r.t.	H ₂ /1 atm	100	This work
2	Pd/PPh ₃ @FDU-12 (8.33 × 10 ⁻⁴ mmol Pd)	1 h	EtOH	40	H ₂ /10 bar	99	[40]
3	PdNP(0.5%)/Al ₂ O ₃ (0.3 g)	3 h	THF	r.t.	H ₂ /1 atm	100	[41]
4	Pd-(CH ₃) ₂ NHBH ₃ (6 mol%)	10 min	H ₂ O/MeOH	r.t.	(CH ₃) ₂ NHBH ₃	99	[42]
5	PdCu/graphene (2 mol% Pd)	1.5 h	H ₂ O/EtOH	50	NaBH ₄	98	[43]
6	APSNP ^a (1 mol%)	2 h	EtOH	r.t.	H ₂ /40 atm	100	[44]
7	Pd/graphene	1.5 h	H ₂ O/EtOH	50	NaBH ₄	91	[43]
8	PdCu/C (2 mol% Pd)	1.5 h	H ₂ O/EtOH	50	NaBH ₄	85	[43]
9	Pd@Hal/di-urea ^b (1.5 wt%)	1 h	H ₂ O	50	H ₂ /1 bar	100	[45] ⁴⁰

^a activated palladium sucrose nanoparticles.^b Pd immobilized on functionalized Hal.**Fig. 7.** The recyclability of Pd@Hal-CCD for hydrogenation of nitrobenzene under optimized reaction condition.

terms of green chemistry criteria. Moreover, the protocols that proceed using low hydrogen pressure are safer and more cost effective. On the other hand, use of non-toxic solvents is very environmentally friendly and more interesting comparing to use of hazardous solvents such as THF. Regarding the reaction temperature, the protocols that could proceed at low temperature could be less expensive. Hence, it can be concluded that Pd@Hal-CCD that led to the desired product in relatively short reaction time and in aqueous media at ambient temperature can be considered as an efficient catalyst. Apart from high efficiency of Pd@Hal-CCD, use of naturally occurring biocompatible raw materials for the synthesis of the catalyst as well as simple preparation method rendered Pd@Hal-CCD a good candidate for catalysis.

3.1. Catalyst recyclability

The recyclability of Pd@Hal-CCD for the hydrogenation of nitrobenzene was investigated, Fig. 7. It was found that Pd@Hal-CCD had the capability of reusing for six reaction runs. More precisely, after each reaction run a slight loss of the catalytic activity was observed. The ICP analysis of the recycled Pd@Hal-CCD after six reaction runs confirmed slight leaching of Pd nanoparticles (only 3 wt% of the initial Pd loading).

4. Conclusion

In a nutshell, a novel nanocomposite, Hal-CCD, was developed through hydrothermal treatment of Hal and as-prepared CCD, derived from hydrothermal and carbonization of CD. The nanocomposite was then palladated through wet impregnation

method and applied as a heterogeneous catalyst for promoting hydrogenation of nitroarenes. The results confirmed high catalytic activity, selectivity and recyclability of the catalyst. To elucidate the role of CCD and Hal in the catalysis, two control catalysts, Pd@Hal and Pd@CCD were prepared and their catalytic activities were compared with that of the catalyst. The result confirmed the higher catalytic activity of the latter, which was attributed to the higher Pd loading and water disperse ability of the catalyst. The investigation of the ratio of Hal:CCD confirmed that this was an effective parameter on the catalytic activity and the best performance was observed with the ratio of 1:2.

Acknowledgments

The authors appreciate the partial supports from Iran Polymer and Petrochemical Institute and Alzahra University and INSF.

Appendix A. Supplementary data

Supplementary data to this article can be found online at <https://doi.org/10.1016/j.poly.2019.114210>.

References

- [1] Y. Zhang, H. Yang, Co₃O₄ nanoparticles on the surface of halloysite nanotubes, *Phys. Chem. Miner.* 39 (2012) 789–795.
- [2] Y. Zhang, J. Ouyang, H. Yang, Metal oxide nanoparticles deposited onto carbon-coated halloysite nanotubes, *Appl. Clay Sci.* 95 (2014) 252–259.
- [3] Y. Lvov, A. Panchal, Y. Fu, R. Fakhruddin, M. Kryuchkova, S. Batasheva, A. Stavitskaya, A. Glotov, V. Vinokurov, Interfacial self-assembly in halloysite nanotube composites, *Langmuir* 35 (2019) 8646–8657.
- [4] A. Glotov, A. Stavitskaya, Y. Chudakov, E. Ivanov, W. Huang, V. Vinokurov, A. Zolotukhina, A. Maximov, E. Karakhanov, Y. Lvov, Mesoporous metal catalysts templated on clay nanotubes, *Bull. Chem. Soc. Jpn.* 92 (2019) 61–69.
- [5] G. Lazzara, G. Cavallaro, A. Panchal, R. Fakhruddin, A. Stavitskaya, V. Vinokurov, Y. Lvov, An assembly of organic-inorganic composites using halloysite clay nanotubes, *Curr. Opin. Colloid Interface Sci.* 35 (2018) 42–50.
- [6] V. Vinokurov, A. Glotov, Y. Chudakov, A. Stavitskaya, E. Ivanov, P. Gushchin, A. Zolotukhina, A. Maximov, E. Karakhanov, Y. Lvov, Core/shell ruthenium – halloysite nanocatalysts for hydrogenation of phenol, *Ind. Eng. Chem. Res.* 56 (2017) 14043–14052.
- [7] V.A. Vinokurov, A.V. Stavitskaya, E.V. Ivanov, P.A. Gushchin, D.V. Kozlov, A.Y. Kurenkova, P.A. Kolinko, E.A. Kozlova, Y.M. Lvov, Halloysite nanoclay based CdS formulations with high catalytic activity in hydrogen evolution reaction under visible light irradiation, *ACS Sustainable Chem. Eng.* 5 (2017) 11316–11323.
- [8] V. Vinokurov, A. Stavitskaya, A. Glotov, A. Ostudin, M. Sosna, P. Gushchin, Y. Darrat, Y. Lvov, Halloysite nanotube-based cobalt mesocatalysts for hydrogen production from sodium borohydride, *J. Solid State Chem.* 268 (2018) 182–189.
- [9] P. Pasbakhsh, G.J. Churchman, *Natural Mineral Nanotubes*, Apple Academic Press, 2015.
- [10] H. Zhu, M.L. Du, M.L. Zou, C.S. Xu, Y.Q. Fu, Green synthesis of Au nanoparticles immobilized on halloysite nanotubes for surface-enhanced Raman scattering substrates, *Dalton Trans.* 41 (2012) 10465–10471.
- [11] M. Massaro, C.G. Colletti, G. Lazzara, S. Milioto, R. Noto, S. Riela, Halloysite nanotubes as support for metal-based catalysts, *J. Mater. Chem. A* 5 (2017) 13276–13293.
- [12] S. Sadjadi, M. Akbari, B. Léger, E. Monflier, M.M. Heravi, Eggplant-derived biochar-halloysite nanocomposite as supports of Pd nanoparticles for the

- catalytic hydrogenation of nitroarenes in the presence of cyclodextrin, *ACS Sustain. Chem. Eng.* 7 (2019) 6720–6731.
- [13] S. Sadjadi, M. Atai, Ternary hybrid system of halloysite nanotubes, polyacrylamides and cyclodextrin: an efficient support for immobilization of Pd nanoparticles for catalyzing coupling reaction, *Appl. Clay Sci.* 153 (2018) 78–89.
- [14] M. Massaro, V. Schembri, V. Campisciano, G. Cavallaro, G. Lazzara, S. Milioto, R. Noto, F. Parisi, S. Riela, Design of PNIPAAm covalently grafted on halloysite nanotubes as a support for metal-based catalysts, *RSC Adv.* 6 (2016) 55312–55318.
- [15] N.T. Thanh Chau, S. Handjani, J.P. Guegan, M. Guerrero, E. Monflier, K. Philippot, A. Denicourt-Nowicki, A. Roucoux, Methylated β -cyclodextrin-capped ruthenium nanoparticles: synthesis strategies, characterization, and application in hydrogenation reactions, *Chem. Cat. Chem.* 5 (2013) 1497–1503.
- [16] S. Manivannan, R. Ramaraj, Synthesis of cyclodextrin-silicate sol-gel composite embedded gold nanoparticles and its electrocatalytic application, *Chem. Eng. J.* 210 (2012) 195–202.
- [17] R. Bleta, S. Noel, A. Addad, A. Ponchela, E. Monflier, Mesoporous RuO₂/TiO₂ composites prepared by cyclodextrin-assisted colloidal self-assembly: towards efficient catalysts for the hydrogenation of methyl oleate, *RSC Adv.* 6 (2016) 14570–14579.
- [18] S. Noël, B. Légera, A. Ponchel, F. Hapiot, E. Monflier, Effective catalytic hydrogenation of fatty acids methyl esters by aqueous rhodium(0) nanoparticles stabilized by cyclodextrin-based polymers, *Chem. Eng. Trans.* 37 (2014) 337–342.
- [19] E. Ozyilmaz, S. Sayin, M. Arslan, M. Yilmaz, Improving catalytic hydrolysis reaction efficiency of sol-gel-encapsulated *Candida rugosa* lipase with magnetic β -cyclodextrin nanoparticles, *Colloids Surf. B* 113 (2014) 182–189.
- [20] S. Manuel, B. Léger, A. Addad, E. Monflier, F. Hapiot, Cyclodextrins as effective additives in AuNPs-catalyzed reduction of nitrobenzene derivatives in a Ball-Mill, *Green Chem.* 18 (2016) 5500–5509.
- [21] Y.-Y. Chu, Z.-B. Wang, Z.-Z. Jiang, D.-M. Gu, G.-P. Yin, A novel structural design of a Pt/C-CeO₂ catalyst with improved performance for methanol electro-oxidation by β -cyclodextrin carbonization, *Adv. Mater.* 23 (2011) 3100–3104.
- [22] W. Zhu, T. Liu, W. Chen, X. Liu, Fast preparation of fluorescent carbon nanoparticles from β -cyclodextrin via precursor design treatment, *Mater. Lett.* 139 (2015) 122–125.
- [23] E.S. Da Silva, N.M.M. Moura, A. Coutinho, G. Drazic, B.M.S. Teixeira, N.A. Sobolev, C.G. Silva, M.G.P.M.S. Neves, Manuel Prieto, J.L. Faria, Beta-cyclodextrin as a precursor to holey C-doped g-C₃N₄ nanosheets for photocatalytic hydrogen generation, *Chem. Sus. Chem.* 11 (2018) 2681–2694.
- [24] E.A. Gelder, S.D. Jackson, C.M. Lok, The hydrogenation of nitrobenzene to aniline: a new mechanism, *Chem Commun.* (2005) 522–524.
- [25] N. Bouchenafa-Saib, P. Grange, P. Verhasselt, F. Addoun, V. Dubois, Effect of oxidant treatment of date pit active carbons used as Pd supports in catalytic hydrogenation of nitrobenzene, *Appl. Catal. A* 286 (2005) 167–174.
- [26] X. Yu, M. Wang, H. Li, Study on the nitrobenzene hydrogenation over a Pd-B/SiO₂ amorphous catalyst, *Appl. Catal. A* 202 (2000) 17–22.
- [27] R. Giordano, P. Serp, P. Kalck, Y. Kihn, J. Schreiber, C. Marhic, J.L. Duvail, Preparation of rhodium catalysts supported on carbon nanotubes by a surface mediated organometallic reaction, *Eur. J. Inorg. Chem.* 2003 (2003) 610–617.
- [28] C.-H. Li, Z.-X. Yu, K.-F. Yao, S.-F. Ji, J. Liang, Nitrobenzene hydrogenation with carbon nanotube-supported platinum catalyst under mild conditions, *J. Mol. Catal. A: Chem.* 226 (2005) 101–105.
- [29] N. Arora, A. Mehta, A. Mishra, S. Basu, 4-Nitrophenol reduction catalysed by Au-Ag bimetallic nanoparticles supported on LDH: homogeneous vs. heterogeneous catalysis, *Appl. Clay Sci.* 151 (2018) 1–9.
- [30] N. Bahri-Laleh, S. Sadjadi, A. Poater, Pd immobilized on dendrimer decorated halloysite clay: computational and experimental study on the effect of dendrimer generation, Pd valence and incorporation of terminal functionality on the catalytic activity, *J. Colloid Interface Sci.* 531 (2018) 421–432.
- [31] S. Sadjadi, M. Akbari, E. Monflier, M.M. Heravi, B. Leger, Pd nanoparticles immobilized on halloysite decorated with a cyclodextrin modified melamine-based polymer: a promising heterogeneous catalyst for hydrogenation of nitroarenes, *New J. Chem.* 42 (2018) 15733–15742.
- [32] S. Sadjadi, M.M. Heravi, M. Malmir, B. Masoumi, HPA decorated halloysite nanoclay: an efficient catalyst for the green synthesis of spirooxindole derivatives, *Appl. Organomet. Chem.* 32 (2018) e4113.
- [33] R. Liu, E. Liun, R. Ding, K. Liu, Y. Teng, Z. Luo, Z. Li, T. Hu, T. Liu, Facile in-situ redox synthesis of hierarchical porous activated carbon@MnO₂ core/shell nanocomposite for supercapacitors, *Ceram. Int.* 4 (2015) 12734–12741.
- [34] S. Sadjadi, M. Atai, Palladated halloysite hybridized with photo-polymerized hydrogel in the presence of cyclodextrin: an efficient catalytic system benefiting from nanoreactor concept, *Appl. Organomet. Chem.* 33 (2019) e4776.
- [35] J. Jin, L. Fu, H. Yang, J. Ouyang, Carbon hybridized halloysite nanotubes for high-performance hydrogen storage capacities, *Sci. Rep.* 5 (2015) 12429.
- [36] A. Arenaza-Corona, D. Morales-Morales, I.F. Hernández-Ahuactzi, V. Barba, Structural and conformational changes in [M(1,10-diaza-18-crown-6)Cl₂] (M = Pd, Pb) complexes: a crystallographic and theoretical study, *CrystEngComm* 20 (2018) 6733–6740.
- [37] S. Bordeepong, D. Bhongsuwan, T. Pungrassami, T. Bhongsuwan, Characterization of halloysite from Thung Yai District, Nakhon Si Thammarat Province, in Southern Thailand, *Songklanakaraj J. Sci. Technol.* 33 (2011) 599–607.
- [38] L. Zatta, J.E.F. da Costa Gardolinski, F. Wypych, Raw halloysite as reusable heterogeneous catalyst for esterification of lauric acid, *Appl. Clay Sci.* 51 (2011) 165–169.
- [39] S. Sadjadi, M.M. Heravi, M. Malmir, Pd@HNTs-CDNS-g-C₃N₄: a novel heterogeneous catalyst for promoting ligand and copper-free Sonogashira and Heck coupling reactions, benefits from halloysite and cyclodextrin chemistry and g-C₃N₄ contribution to suppress Pd leaching, *Carbohydr. Polym.* 186 (2018) 25–34.
- [40] M. Guo, H. Li, Y. Ren, X. Ren, Q. Yang, C. Li, Improving catalytic hydrogenation performance of Pd nanoparticles by electronic modulation using phosphine ligands, *ACS Catal.* 8 (2018) 6476–6485.
- [41] S. Agrahari, S. Lande, V. Balachandran, G. Kalpana, R. Jasra, Palladium supported on mesoporous alumina catalyst for selective hydrogenation, *J. Nanosci. Curr. Res.* 2 (2017), 2572–0813.1000114.
- [42] N.M. Patil, M.A. Bhosale, B.M. Bhanage, Transfer hydrogenation of nitroarenes into anilines by palladium nanoparticles via dehydrogenation of dimethylamine borane complex, *RSC Adv.* 5 (2015) 86529–86535.
- [43] Y.-S. Feng, J.-J. Ma, Y.-M. Kang, H.-J. Xu, PdCu nanoparticles supported on graphene: an efficient and recyclable catalyst for reduction of nitroarenes, *Tetrahedron* 70 (2014) 6100–6105.
- [44] D. Samsonu, M. Brahmayya, B. Govindh, Y. Murthy, Green synthesis & catalytic study of sucrose stabilized Pd nanoparticles in reduction of nitro compounds to useful amines, *S. Afr. J. Chem. Eng.* 25 (2018) 110–115.
- [45] S. Dehghani, S. Sadjadi, N. Bahri-Laleh, M. Nekoomanesh-Haghighi, A. Poater, Study of the effect of the ligand structure on the catalytic activity of Pd@ligand decorated halloysite: combination of experimental and computational studies, *Appl. Organomet. Chem.* (2019) e4891.